

Interactive spatiotemporal modelling of health systems: the SEKS–GUI framework

Hwa-Lung Yu · Alexander Kolovos ·
George Christakos · Jiu-Chiuan Chen ·
Steve Warmerdam · Boris Dev

© Springer-Verlag 2007

Abstract This paper describes the spatiotemporal epistematics knowledge synthesis and graphical user interface (SEKS–GUI) framework and its application in medical geography problems. Based on sound theoretical reasoning, the interactive software library of SEKS–GUI explores heterogeneous (spatially non-homogeneous and temporally non-stationary) health attribute distributions (disease incidence, mortality, human exposure, epidemic propagation etc.); expresses the health system’s dependence structure using (ordinary and generalized) spatiotemporal covariance models; synthesizes core knowledge bases, empirical evidence and multi-sourced system uncertainty; and generates a meaningful picture of the real-world system using space–time dependent probability functions and associated maps of health attributes. The implementation stages of the SEKS–GUI library are described in considerable detail using appropriate screens. The wide applicability of SEKS–GUI is demonstrated by reviewing a selection of real-world case studies.

Keywords Medical geography · Health · Disease · Epidemic · Uncertainty · BME · Interdisciplinary

H.-L. Yu (✉) · G. Christakos · S. Warmerdam · B. Dev
Department of Geography, San Diego State University,
San Diego, CA 92182-4493, USA
e-mail: hlyu@mail.sdsu.edu

A. Kolovos
SAS Institute, Inc., SAS Campus Drive,
Cary, NC 27513, USA

J.-C. Chen
Department of Epidemiology, University of North Carolina,
Chapel Hill, NC 27599, USA

1 Introduction

The study of a health system’s attributes (e.g., mortality pattern, disease propagation velocity, exposure distribution, and system performance indicators) is an important affair in medical geography that can play a vital role in a large number of public health situations, including population risk analysis, public awareness, health policy and decision making (Haggett 2000; Cromley and McLafferty 2002; Gatrell 2002). A health system typically involves a number of interacting agents and the associated knowledge bases (Christakos and Hristopulos 1998). In this context, some of the health attributes of interest are emergent properties that manifest the composite geographical-temporal organization of the system. The study of a health system may cross disciplines and is basically a knowledge synthesis affair that combines (a) a stochastic theory of space–time dependence representation under conditions of multi-sourced uncertainty with (b) an epistematics methodology that is the fusion of human teleology and evolutionary epistemology.

The spatiotemporal random field (S/TRF) model of stochastics aims to study the properties of a health system as a whole and connect them to causal relations and space–time patterns under conditions of uncertainty. S/TRF tools include spatiotemporal probability density functions (PDF), ensemble averages (ordinary and generalized covariance and variogram functions), and local scale heterogeneity characteristics (spatial and temporal orders). A detailed presentation of stochastics, in general, and the S/TRF model, in particular, can be found in Christakos (1991, 1992), Christakos and Hristopulos (1998) discuss several of its applications in health sciences. Epistematics involves models of the processes (perceptual, intellectual and linguistic) by which knowledge and understanding are

achieved and communicated; these models include both mental constructions of the actual health system and the general conditions of the mind that enable scientists to develop different disciplines that operate in an autonomous way but allow disciplinary integration to obtain a realistic world view (Knorr Cetina 1999; Keil and Wilson 2000; Meyer and van der Hoek 2004; Rescher 2005; Christakos et al. 2005).

Ultimately, much medical geography research strives to develop integrated health systems to aid in innovative inquiry and interdisciplinary problem solving, effectively joining communities of scholars from different fields of study. For these efforts to succeed, practicing scientists, scholars and research administrators from a range of disciplines should be interested in creating and working in environments that support traversing of intellectual, cultural, and organizational boundaries. By capitalizing on interdisciplinary knowledge synthesis, medical geography research emphasizes the importance of multiple focuses and perspectives in scientific investigations, including the development of interactive software libraries of spatiotemporal modelling and mapping.

2 The SEKS–GUI software library

Space–time data analysis in a modern statistical framework was introduced by Christakos (1990, 1991, 1992). Subsequent developments include the works of Goodall and Mardia (1994), Haas (1995), Bogaert (1996), Serre et al. (1998), Kyriakidis and Journel (1999), and Cressie and Huang (1999). More recent works include Ma (2003), Kolovos et al. (2004), Stein (2005), and Porcu et al. (2006); see the relevant spatiotemporal statistics literature.

The study of many medical geography problems is essentially a knowledge synthesis affair that, generally, involves four major stages: adequate conceptualization, rigorous formulation, substantive interpretation, and innovative implementation. Each stage requires the interdisciplinary effort of individuals familiar and receptive to important science integration goals, extensively discussed in the public health literature (Gatrell 2002; Christakos et al. 2005; Ebi et al. 2005). The SEKS–GUI computer software library (spatiotemporal epistematics knowledge synthesis graphical user interface; for the most recent user manual, see Kolovos et al. 2006) is used in the implementation stage of knowledge synthesis. Let $X_p = X(\mathbf{p})$ denote a health attribute, where $\mathbf{p} = (s, t)$ is a point in the space–time domain (the vector s denotes the geographical location and the scalar t denotes the time under consideration). SEKS–GUI is primarily a spatiotemporal modelling and mapping library that includes:

- Stochastic models of composite space–time dependence, uncertainty representation, and data assimilation (Table 1).
- Spatiotemporal covariance models of X_p (ordinary, c_X , and generalized, κ_X) for health systems with different kinds of correlation structure (Table 2).
- Varying levels of continuity orders (ν and μ) expressing heterogeneities in the spatial and temporal patterns of the health attribute X_p (Table 2).
- Mapping techniques with attractive features from a theoretical and an applied perspective (Table 4).

Table 1 roughly categorizes the stochastic models providing the theoretical support of the SEKS–GUI in terms of spatiotemporal dependence, uncertainty representation and data assimilation criteria. In addition to the considerable number of covariance models mentioned in Table 2, there are other classes of models (Kolovos et al. 2004) that can be included in the SEKS–GUI framework. Noteworthy elements of SEKS–GUI are its generalization powers that account for space–time heterogeneous dependence, non-Gaussian probability laws and non-Bayesian data assimilation (Table 4). Many well-known ontologic predictors are based on the minimum prediction variance criterion and are often subject to linearity and Gaussian assumptions, whereas the SEKS–GUI predictors are based on maximum information and adaptation principles and are, in general, nonlinear (a list of predictors is given in Table 3). Another significant advantage of this group of techniques is the systematic generation of complete PDF at all mapping points (Fig. 1) rather than a single value for the health attribute under consideration. In fact, many ontologic techniques can be derived as special cases of the more general epistematics framework.

For illustration, we consider two techniques currently used in SEKS–GUI: the BME (Bayesian maximum entropy) and the GBME (generalized BME), see Tables 3 and 4 (a detailed description of these techniques and their real-world applications can be found in the relevant literature, including Christakos and Bogaert 1996; Christakos 2000; Douaik et al. 2004, 2005; Quilfen et al. 2004; Law et al. 2006; Wibrin et al. 2006; Yu and Christakos 2006; Orton and Lark 2007). Both techniques are based on epistematics ideals seeking a maximally informative model of the attribute map subject to the available general (core) knowledge; subsequently, each technique assimilates site-specific knowledge by means of conditional (or adaptation) principles. In practice, data-detrending and transformation operators may be used in BME implementation, yielding spatially homogeneous and temporally stationary attribute representations. The GBME technique directly accounts for heterogeneous and non-Gaussian data distributions, which means that transformation and detrending operators are not

Table 1 A categorization of stochastic models by spatiotemporal dependence, uncertainty representation and data assimilation criteria

Spatiotemporal dependence	Uncertainty representation	Data assimilation
Homogeneous/ stationary: ordinary S/TRF theory	Gaussian probability laws	Bayesian conditional rules (operational)
Non-homogeneous/ non-stationary: generalized S/TRF theory	Non-Gaussian probability laws	Non-Bayesian adaptation principles (stochastic logic)

Table 2 Examples of space–time covariance models

Spatiotemporal dependence	Separable models	Non-separable models
Homogeneous/stationary	$\sum_q c_{p,q}(r)$ and $\sum_q c_{p',q}(\tau)$	$\sum_{q=1}^2 c_{p,q}(r) c_{p',q}(\tau)$
Non-homogeneous/ non-stationary	$c_{p,1}(r) c_{p',1}(\tau)$	$c_p(\mathbf{r} + \mathbf{u}\tau)$ $\kappa(r, \tau)$ ν, μ

Note The functions $c_{p,q}(r)$, $p = 1, \dots, 7$ and q is a non-negative integer, represent the spatial exponential ($p = 1$), Gaussian ($p = 2$), spherical ($p = 3$), sine ($p = 4$), cosine ($p = 5$), and Mexican-hat ($p = 6$) and nugget-effect ($p = 7$) model; and the $c_{p',q}(\tau)$, $p' = 8, \dots, 14$, represent the temporal exponential ($p' = 8$), Gaussian ($p' = 9$), spherical ($p' = 10$), sine ($p' = 11$), cosine ($p' = 12$), Mexican-hat ($p' = 13$) and nugget-effect ($p' = 14$) models; the r and τ denote the spatial and the temporal lag, respectively. The functions $c_p(\mathbf{r} + \mathbf{u}\tau)$ represent the composite space–time exponential ($p = 1$), Gaussian ($p = 2$) and polynomial-exponential ($p = 3$) models; \mathbf{r} is the vector distance and \mathbf{u} is a propagation speed. The $\kappa(r, \tau)$ is the polynomial generalized covariance of orders ν (spatial) and μ (temporal)

Table 3 A classification of mapping techniques

Ontologic spatiotemporal techniques	Epistematics spatiotemporal techniques
STK (spatiotemporal kriging)	BME (Bayesian maximum entropy)
GSTK (generalized spatiotemporal kriging)	GBME (generalized BME)
KF (Kalman filter)	MBME (Material biconditional ME)
	GMBME (Generalized MBME)

needed. For both techniques, numerical codes have been developed and bundled into a user interface creating an easy-to-use SEKS–GUI framework. This framework addresses the needs of users with multidisciplinary backgrounds, without imposing any programming requirements.

The spatiotemporal modelling codes are unified within the GUI framework such that the SEKS–GUI comprehensively features:

Table 4 Some features of the BME and GBME mapping techniques

Space–time dependence representation	Site-specific knowledge assimilated
Heterogeneous, in general (homogeneous-stationary are special cases)	Hard data and soft (uncertain) information
<i>Predictor</i>	<i>Prediction maps</i>
Non-linear, in general (linear is special case)	Complete PDF at each space–time grid point
	Joint PDF at several points
	Mean, mode, and median at each point
<i>Underlying probability laws</i>	<i>Accuracy maps</i>
Non-Gaussian, in general (Gaussian is special case)	Error variance, std. deviation, skewness, and confidence intervals
<i>General (core) knowledge processed</i>	<i>Forthcoming</i>
Theoretical models, scientific laws, and empirical relations	Multi-attribute (Vector) mapping
	Functional (change-of-support) mapping

- The theoretical support of interdisciplinary synthesis, operational conditionals, stochastic logic and generalized random fields.
- A user-friendly interface with screens that facilitate space–time data modelling and mapping and allow users to control each stage of their investigation.
- Built-in functions so that users need to neither handle individual library functions nor connect the processing software steps. Since these steps appear seamless, users can concentrate on substantive modelling activities.
- A complete graphics-based environment that offers significant flexibility in providing the input, deciding the investigation course, choosing among an array of predictors, and selecting from a broad variety of output visualization options.

The above features, combined with the unique characteristics of the knowledge synthesis methodology implemented in the software libraries supporting the interface,

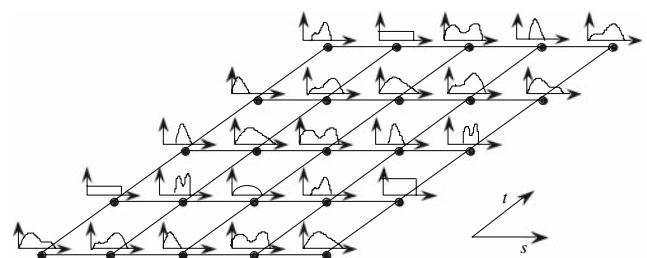


Fig. 1 An illustration of a set of health attribute PDF that vary across space–time

make SEKS–GUI a useful addition to the spectrum of analysis and interpretation tools of modern geographic information science (GIS).

3 A brief tour of SEKS–GUI

SEKS–GUI is designed around a sequence of consecutive screens that guide users through the main phases of spatiotemporal modelling and mapping. Each screen constitutes a modelling advancement by itself, in the sense that when reaching its end the user has completed successfully a different investigation stage. Users actively participate by inserting data files, providing insight about the data, selecting meaningful space–time correlation ranges and prediction parameters, and expressing preferences concerning the mode of attribute mapping and the associated visualization means. Issues unrelated to substantive investigation require minimal effort, buttons and drop-menus facilitate case-related decisions, a broad range of informative space–time maps can be readily generated, and brief explanations and tool-tips are provided “on the spot”. Individual screens are built to resemble a wizard-type of set-up, in the sense that users can easily provide their input or make alternative choices according to the needs of their investigation.

A comprehensive user manual addresses a broad range from the novice user to the field expert. Naturally, the preparation of input data is required prior to using the SEKS–GUI. This initial action involves compiling, gathering and rendering data in forms that can be employed by the interface. Also, since attribute predictions will be produced at specified spatiotemporal grid nodes, the user must define a suitable mapping grid (see Sect. 3.1).

A brief outline of the main phases of SEKS–GUI is given in Fig. 2. The screens follow a phase progression that is contingent on the spatiotemporal technique implemented. For the BME technique, we consider five phases: definition of investigation type and provision of input information; space–time exploratory analysis; separable and non-separable covariance modeling; systematic prediction of the health attribute at all grid nodes; and visualization of the results. The GBME technique, on the other hand, consists of fewer (four) phases, since the space–time (generalized) covariance modelling is intrinsically performed at the prediction phase. In addition, a shorter sequence of screens is required at the exploratory phase.

3.1 Phase 1: Supplying the information

Initially, the users are asked to choose between the BME and the GBME techniques. Inputs at this phase include,

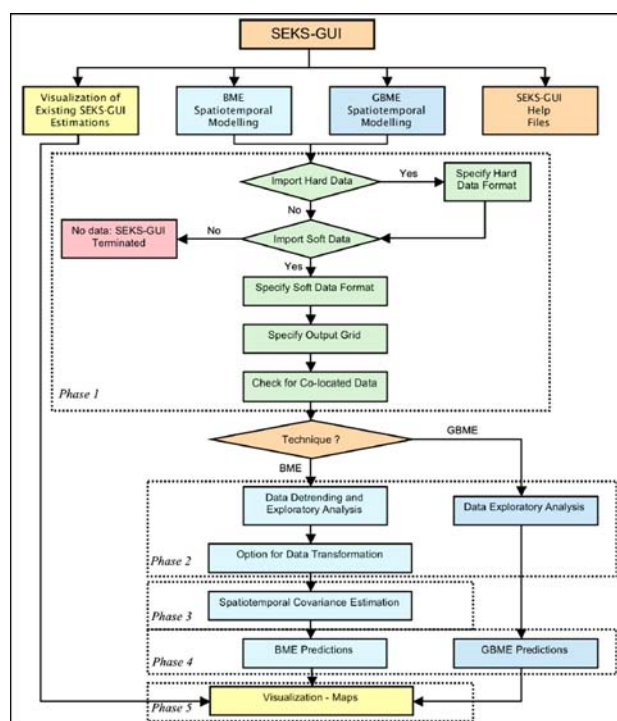


Fig. 2 Brief outline of the main SEKS–GUI phases

directly or indirectly, the general (core) and the site-specific knowledge bases, as well as information regarding specifics of the space–time mapping grid. In most medical geography applications, core knowledge may be available in the form of:

- Theoretical covariance models (ordinary or generalized) known to adequately describe the general correlation structure of a certain range of health systems. Theoretical models are included in the SEKS–GUI list of covariance models (Table 2; SEKS–GUI is continuously updated to include new models).
- Natural laws, scientific relationships and empirical charts that are relevant to the health system attributes. Depending on the situation, such information may be used to derive the corresponding covariance model, which can then be added to the list of models (e.g., an exposure law leads to the corresponding covariance equation, which is solved yielding a physically meaningful theoretical model).

Research studies have shown that, depending on the situation, the SEKS–GUI framework can integrate natural laws, exposure–population effect associations, epidemic relations, and carcinogenesis models expressed in a stochastic form (Serre and Christakos 1999; Christakos and Kolovos 1999; Kolovos et al. 2002; Serre et al. 2003; Quilfen et al. 2004; Christakos et al. 2002, 2004, 2005).

Automatic incorporation of core knowledge in SEKS–GUI by means of interactive screens is a major area of ongoing research and development.

A site-specific knowledge base, on the other hand, can be conveniently split into two major sub-categories:

- Hard data, i.e. measurements and observations that are characterized by a satisfactory level of accuracy and are expressed as numerical attribute values across space–time.
- Soft data, i.e. measurements and observations that include a significant amount of uncertainty that cannot be ignored. Soft data may have the form of interval values and (Gaussian, triangular, uniform or custom-defined) distributions that approximate local or global data uncertainties (Fig. 3).

A sequence of SEKS–GUI screens serves the purpose of accepting data based on the knowledge bases described above. A core base that includes theoretical covariance models is considered in Phase 1, whereas model parameter estimation uses site-specific knowledge bases (Sect. 3.3 below). Hard and soft data inputs are acceptable in both Text and Excel-formatted spreadsheet files (Fig. 4); the users also select a Text or an Excel-formatted file to define space–time coordinates for the output nodes.

3.2 Phase 2: Exploratory analysis

The second sequence of SEKS–GUI screens evaluates the knowledge bases to be used in the investigation. Because duplicate coordinates (co-located data) may result in covariance matrix singularities, the matter is considered carefully in SEKS–GUI (see Appendix A). Depending on the spatiotemporal technique, the SEKS–GUI follows different paths. The GBME technique allows the input information to be forwarded directly to the prediction phase (Sect. 3.3 below).

The BME technique, on the other hand, requires additional exploratory work, since the corresponding prediction phase uses a detrended-normally distributed dataset. Applying a Gaussian kernel on the dataset detrends it: the kernel searches for neighboring data within user-defined ranges of the spatiotemporal domain and extracts the trend

using a smoothing moving window. However, because any extreme values could bias the moving window, trend estimates may be drastically affected. SEKS–GUI addresses the matter by identifying potential outliers in the datasets and isolating them from the detrending process. Extreme outliers are excluded from data trend calculations using criteria based on box plot graphical techniques (Box et al. 1994). Outliers, if any, are not excluded from the prediction process; in fact, the original dataset is left unaltered for the prediction phase. Mean trend calculations use attribute values usually represented by hard data, but the dataset may contain limited (or no) hard data, in which case SEKS–GUI resolves the issue by employing soft data in trend calculation, as well. Figure 5 displays the detrending screen for BME. Once the spatiotemporal trend has been calculated, it is used to detrend the soft data, as well. The final stage of Phase 2 is to assess data normality. Using both the hard values and the soft approximations as the detrended dataset, the SEKS–GUI compares its cumulative distribution function (CDF) versus the Gaussian one with the detrended data mean and variance. In the corresponding screen (Fig. 6), the user decides whether the data will undergo a transformation from their original space into a space where their distribution will resemble a Gaussian one. SEKS–GUI offers the transformation options discussed in Appendix B.

To summarize Phase 2, detrended data are manipulated to comply with the requirements of the prediction phase. Various alternatives can be tried to optimally handle the available information, and each alternative transforms the detrended dataset of the original space into a different set of values. Note that varying dynamics may develop within the dataset as a result of these manipulations. Based on suggestions made by Olea (2006), a transformation is automatically suggested when the maximum deviation of the detrended distribution from normality is larger than 10% etc.

3.3 Phase 3: Spatiotemporal covariance analysis

This third sequence of screens in the SEKS–GUI deals with the investigation of spatiotemporal correlation patterns that characterize the attribute distribution.

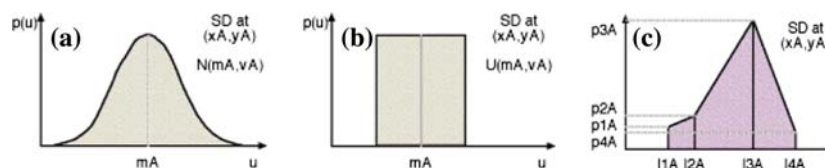


Fig. 3 Drawings of soft data (SD) at the spatial coordinates (xA,yA) used in SEKS–GUI: **a** Gaussian distribution for attribute u with mean m_A and variance v_A . **b** Uniform distribution (m_A, v_A). **c** A user-

defined distribution (the datum PDF has three bins with limits are I_{1A}, I_{2A}, I_{3A} and I_{4A} ; within each bin the PDF changes linearly between the values p_{1A}, p_{2A}, p_{3A} and p_{4A})

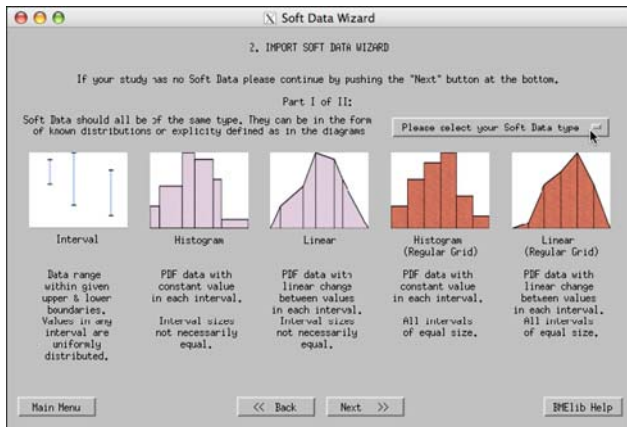


Fig. 4 A screenshot of the soft data wizard in SEKS-GUI, at the stage of providing the soft information

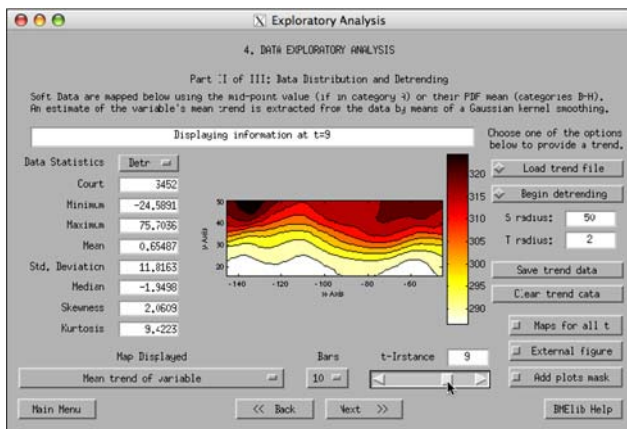


Fig. 5 A screenshot of the detrending screen at the exploratory analysis stage of the BME version. The *map* displayed is the mean trend of the total ozone distribution over US on July 9, 1998, as calculated within SEKS-GUI

If the BME technique is selected, three steps are required as follows:

- Divide the domain under consideration into an appropriate number of space–time neighborhoods based on the user’s insight, the geographical constraints, and the spatiotemporal distribution of the data available.
- Use BME for each space–time neighborhood. Within the neighborhood, explore different classes of spatial and temporal distances (lags) between data points and calculate experimental (sample or raw) covariance values for each lag class.
- Fit a model to the experimental covariance values of step *a* to obtain a closed-form expression of the attribute dependence across space–time.

As in the detrending stage of exploratory analysis, point values are used. The covariance of the soft data can be

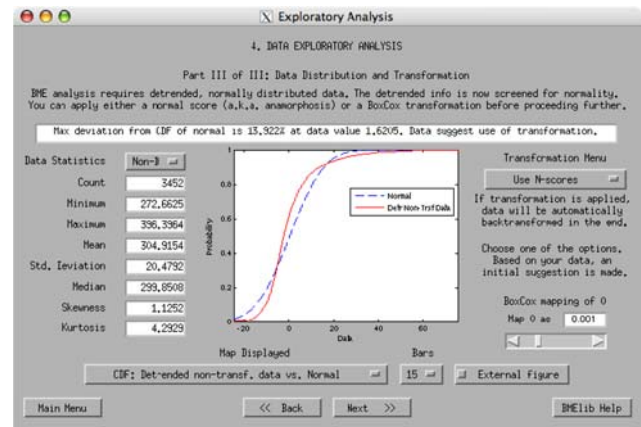


Fig. 6 A screenshot of the data transformation screen at the exploratory analysis stage of the BME version. The plot compares the CDF of the detrended user data (*solid line*) and the normal distribution defined by the detrended data distribution mean and variance (*dashed line*). Note that based on this comparison SEKS-GUI suggests use of a data transformation

calculated using soft data means (e.g., interval data mid-points). Accordingly, the SEKS-GUI uses the set consisting of detrended and possibly transformed hard data and soft data approximations. Within each of the space–time neighborhoods [defined in step (a)], the isotropic or anisotropic experimental covariance values are calculated in step (b) based on the user-defined spatial and temporal classes. In step (c), a theoretical covariance model—or a combination of two individual models nested in each other and selected from a list of permissible functions (Table 2)—may be fitted to the available information at each space–time neighborhood. Since this procedure is often based on visual inspection, there may be no single best fit. Instead, the fit will depend on the user’s choice of the parameters and experience with the particular dataset, which may prove more valuable than a strict statistical fitting procedure. The covariance parameters (sill and range) are then adjusted until an optimal fit is reached (both individual and nested models can be considered). An example of fitting a theoretical model to the experimental covariance values is displayed in Fig. 7.

If the GBME technique has been selected, the (generalized) space–time covariance modelling is handled intrinsically at the prediction phase (Sect. 3.4). In particular, the SEKS-GUI automatically tests all permissible combinations of space–time heterogeneity orders (ν and μ) and generalized covariance models (κ_X) within the local neighborhoods by means of cross validation at a set of test points, selecting as optimal the one with the highest average predictive power (for a detailed introduction to the generalized random field theory and its applications, see Christakos 1991, 1992; Christakos and Lai 1997; Yu and Christakos 2006). Note that the κ_X -class is richer than that

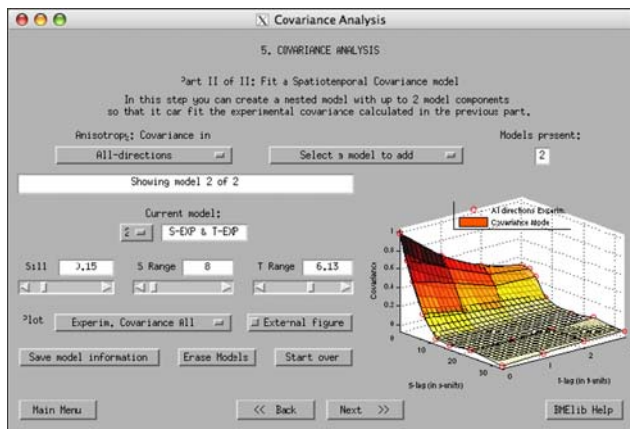


Fig. 7 A screenshot of the covariance analysis phase of the BME version. The plot displays the experimental covariance derived from the data as *circles* connected with the *larger tiles*, and the covariance model fitted to them as the surface with the semi-transparent *smaller tiles*

of ordinary covariances (c_X). The user may decide to obtain visualizations of κ_X at selected regions, given that incorporation of all grid nodes may require large computer storage capabilities.

Spatial and temporal variations are interrelated, as the geographical propagation of an attribute may also be affected by temporal mechanisms. The heterogeneity orders provide a quantitative assessment of the rate of space–time change in attribute patterns and may determine how “far away” in space and “deep” in time the analysis searches for information about the attribute. Not only does the spatial order ν change in space, but the temporal order μ does as well. In the last phase (Sect. 3.5 below), the user may choose to obtain a visual representation of the geographical $\nu - \mu$ distribution, thus gaining information about the relative attribute trends in space–time ($\nu - \mu > 0$ implies higher degree spatial trends; $\nu - \mu < 0$ implies higher degree temporal trends).

3.4 Phase 4: Spatiotemporal prediction

The screens for this phase are similar for both the BME and the GBME techniques. The following options are available when using the BME technique:

- (a) Prediction mode: gives the mode of the prediction PDF at each output space–time grid node, and takes the least amount of time to calculate.
- (b) Prediction moments: generates the mean, variance and skewness coefficient of the prediction PDF at each output grid node.
- (c) Prediction PDF: provides the complete prediction PDF at each grid node, thus requiring more computational power/time to complete than previous options.

- (d) Prediction confidence intervals: in addition to the PDF of the previous option, it offers the confidence interval at a user-preset percentile. Being the most computationally intensive option, this is the most time-consuming of all others.

GBME, on the other hand, can be used to provide only prediction moments [option (b)]. With the exception of option (b), each choice above produces outputs that include the results of the preceding choices (e.g., the calculation of prediction confidence intervals will provide information about the PDF moments). Prior to initiating the prediction process, users can adjust the prediction parameters (such as the maximum number of hard and soft data to be considered at a time) and the estimates of the space–time correlation ranges. Users are also provided with two additional parameters, namely the minimum amount of data to use and the rate at which the data search radius should increase if the quantity of sufficient data is not found in the current neighborhood. The SEKS–GUI continuously informs the users of the prediction progress (Fig. 8 shows a GBME prediction screen), and if a premature interruption occurs, parameter adjustment may be necessary. Typical reasons for interruptions may include singularities in the covariance matrices (suggesting a revision of the covariance model) or limited data availability (suggesting an increase in the maximum number of data considered). If transformations had been applied to the initial dataset, the prediction outcomes are subsequently back-transformed into their original space.

3.5 Phase 5: Visualization

The final phase creates maps based on the outcomes of Phase 4. The users may choose to use the results of Sect. 3.4 or to load an output file with the prediction outcomes from different investigations. The latter option allows the users to advance directly to the visualization

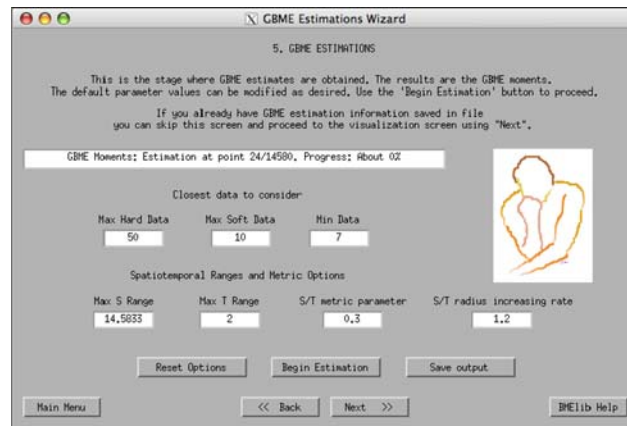


Fig. 8 A screenshot of the prediction phase for the GBME version

screen upon starting to run SEKS-GUI, as mentioned earlier in Sect. 3.1.

Once the prediction outcomes are available, the user can choose from a series of maps, depending on the situation. Specifically, the options include the following types of maps:

- *BME_{mean}* or *GBME_{mean}*. The mean of the prediction PDF at each mapping grid node (Fig. 9)—moments, PDF or confidence intervals are required.
- *BME_{mode}*. The mode of the prediction PDF at each output grid node—modes are required.
- *Prediction error variance*. The variance of the prediction PDF at each output grid node—moments, PDF or confidence intervals required.
- *Prediction standard deviation*. The standard deviation of the prediction PDF at each output grid node—moments, PDF or confidence intervals required.
- *Prediction skewness*. The skewness of the prediction PDF at each output grid node—moments, PDF or confidence intervals required.
- *Prediction PDF*. The prediction PDF are plotted at pre-selected output locations (Fig. 10). The PDF are projected vertically on a map of the grid so that graph cluttering is prevented—PDF or confidence intervals required.
- *Size of the prediction confidence interval*. At each grid node the difference between the attribute values at the limits of the confidence interval is calculated. This map displays the widths of attribute values within which the prediction lies for the confidence level selected by the user—confidence intervals required.
- *Lower and upper limits of the prediction confidence intervals*. These intervals are calculated at each output

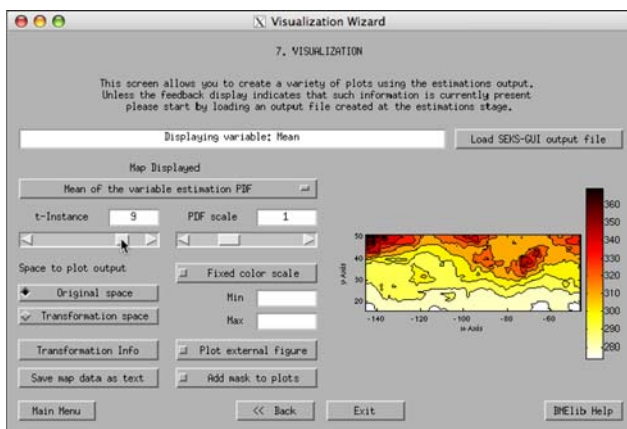


Fig. 9 A screenshot of the visualization phase using the BME version. The *map* displays the predicted total ozone means at the user-defined output grid nodes on July 9, 1998. The map was derived from raw predictions that were back-transformed into the original space and had the trends added back

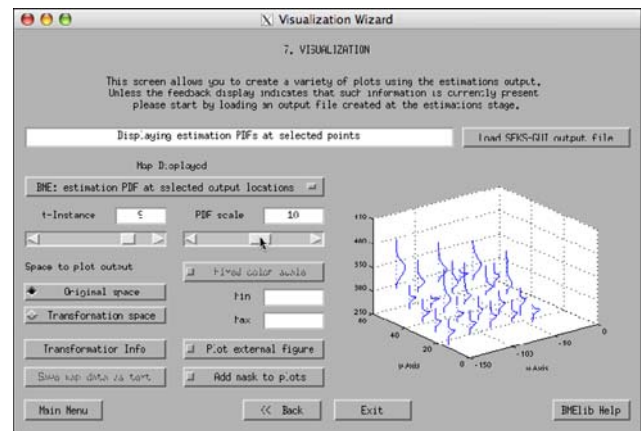


Fig. 10 A screenshot of the visualization stage using the BME version. The *map* displays a collection of predicted total ozone PDF on July 9, 1998 that were back-transformed into the original space with the trend added back. The PDF shown are all on the same scale at selected output locations

- grid node for the confidence level selected by the user—confidence intervals required.
- *Prediction PDF values at the confidence interval limits*. This map represents the corresponding predictions at each grid node—confidence intervals required.
- *Spatial heterogeneity orders*. These are maps of the v and μ orders at each grid node (the v and μ usually take the values 0, 1 or 2)—GBME results required.
- *Space-time heterogeneity differences*. This is a map of $v - \mu$ at each grid node that can take integer values in the ± 2 range (Fig. 11)—GBME results required.

It should be noted that when the BME technique has been selected in a previous phase, the maps in the original space are the back-transformed predictions with the mean trends restored at the prediction locations, when applicable. Additionally, the moment maps are based on the raw prediction PDF moments, which, themselves, have been back-transformed; consequently the mean trends at these locations have been restored. If a transformation has been applied, one can also display maps in the transformation space; basic information regarding the transformation can be also provided. Maps in the transformation space feature detrended data derived directly from the raw predicted PDF. When, instead, the GBME technique has been used, no such issues arise.

3.6 Comments

Although the BME and GBME techniques share the same methodological framework of knowledge synthesis, they exhibit subtle differences in the underlying stochastic theory and the practical implementation features. These matters should be taken into account by the SEKS-GUI users

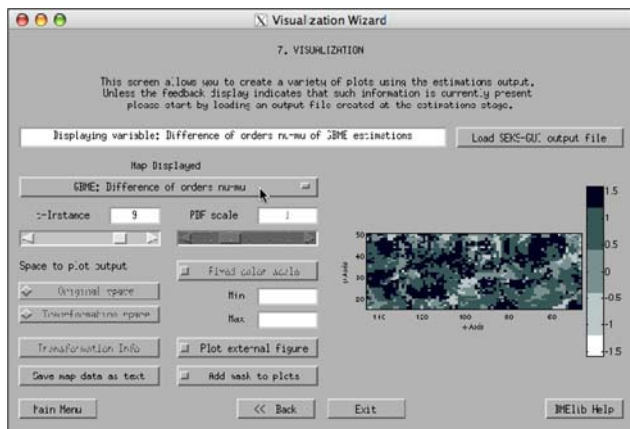


Fig. 11 A screenshot of the visualization phase for the GBME technique. At every grid node the map displays the difference $\nu - \mu$ of the spatial and temporal heterogeneity orders at this node

when they choose between the two techniques. Some of the implementation differences between BME and GBME are briefly discussed in Appendix C (for more information about the two theories and technical details, the interested reader is referred to the relevant literature).

4 Real-world case studies

The SEKS–GUI framework has been implemented in a long list of real-world cases studies. Some of these studies are briefly described in the following subsections, where references to the original works are given for the interested reader.

4.1 Bubonic plague epidemic in India

Yu and Christakos (2006) studied the spatiotemporal evolution of bubonic plague in India during the years 1896–1906 using modern geographical information science techniques. In the past, most investigations focused on selected cities to conduct different kinds of studies, such as the ecology of rats. No detailed maps existed incorporating the space–time dependence structure and sources of uncertainty in the epidemic data, providing a composite space–time picture of the disease propagation characteristics. SEKS–GUI provided the technical means to study the spatiotemporal distribution of bubonic plague under conditions of uncertainty and multi-sourced databases; to incorporate various forms of interdisciplinary knowledge; and to generate informative maps of mortality rates and geographical disease spread as well as epidemic indicator plots, which all provided novel perspectives concerning the distribution and space–time propagation of the deadly epidemic. For illustration, a limited set of mortality maps is shown in Fig. 12. The bubonic plague in India exhibited strong seasonal and geographical features. During its entire

duration, the plague continued to invade new geographical areas, while following a re-emergence pattern at many localities; its rate changed significantly during each year and the mortality distribution exhibited space–time heterogeneous patterns. Combined with indicator plots, mortality maps can make possible the comparison of the propagation patterns of different diseases.

4.2 Black Death epidemic in Europe

For the first time, a series of detailed space–time maps of Black Death characteristics (mortality, infected area propagation, centroid evolution etc.) were obtained throughout the fourteenth century AD Europe (Christakos et al. 2005). The maps integrated a variety of interdisciplinary knowledge bases about the devastating epidemic and provided researchers and the interested public with an informative description of the Black Death dynamics (temporal evolution, local and global geographical patterns and propagation speeds). For illustration, a set of maps representing the total geographical area in Europe infected by Black Death at different times is shown in Fig. 13. The comparative modelling of Black Death in Europe versus bubonic plague in India led to a number of interesting findings (Christakos et al. 2007). Geographical epidemic indicators confirmed that Black Death mortality was two orders of magnitude higher than that of bubonic plague. Modern bubonic plague is a rural disease typically devastating small villages in the countryside, whereas Black Death indiscriminately attacked both large urban centers and the countryside. The epidemics had reverse areal extension features in response to annual seasonal variations (e.g., Fig. 14). During the Indian epidemic, the disease disappeared and reappeared several times at certain locations; in Europe, once the disease entered a place, it lasted for a time proportional to the population and then disappeared for several years. On average, Black Death moved much faster than bubonic plague to reach virgin territories, despite the fact that India is slightly larger in area than western Europe and had a railroad network almost instantly moving infected rats, fleas, and people from one end of the subcontinent to the other. These findings threw new light on the epidemics and need to be taken into consideration in the discussion concerning the two devastating diseases and the lessons learned from them.

4.3 Human exposure due to Chernobyl fallout in Ukraine

The vast territories radioactively contaminated during the 1986 Chernobyl accident (in former Soviet Union-Ukraine) provide a substantial dataset of radioactive monitoring data, which can be used for the verification and testing of

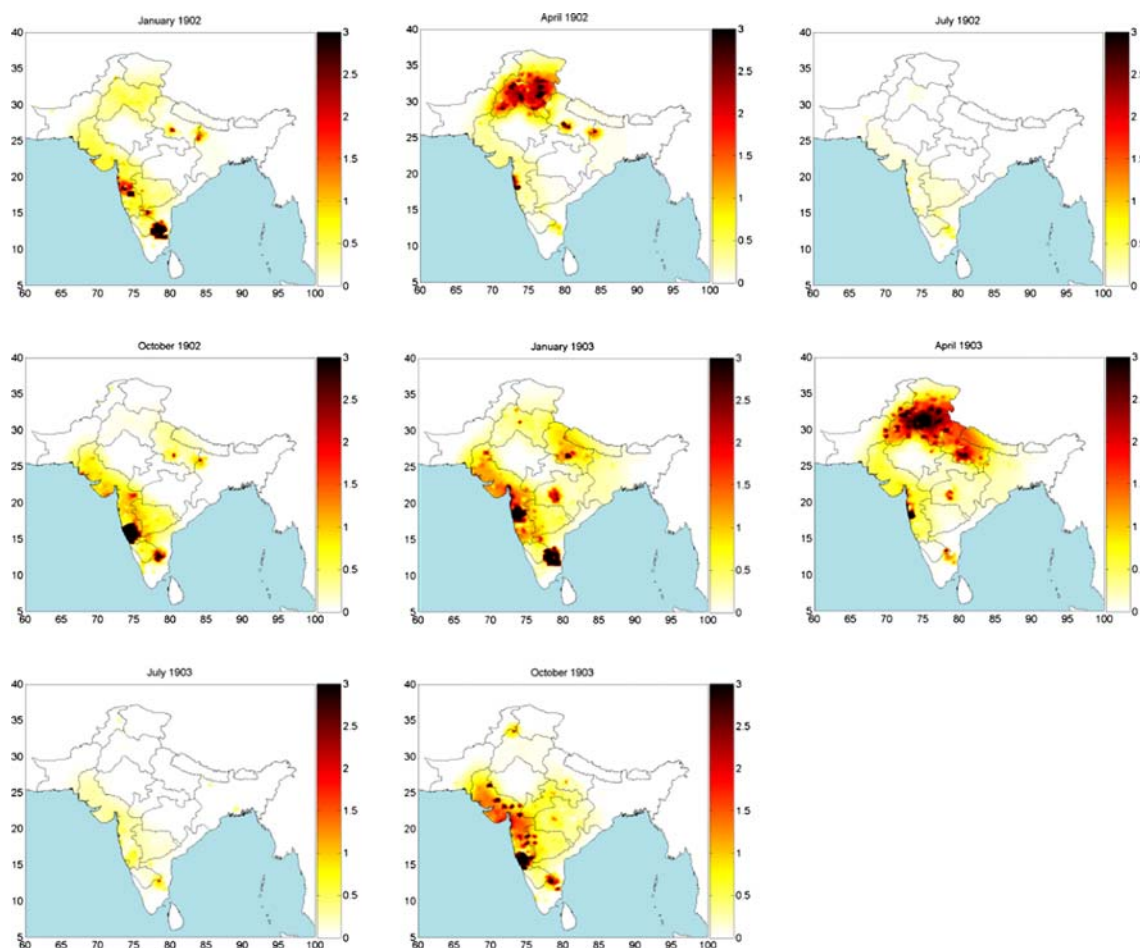


Fig. 12 Space–time mortality rate maps (%) of bubonic plague in India during 1902–1903

health risk assessment methods. Using the Chernobyl dataset for such a purpose was motivated by its geographical structure (large-scale correlations, short-scale variability, spotty features etc.). The BME technique estimated the extent and magnitude of the radioactive soil contamination by ^{137}Cs , which allowed incorporation of a wide variety of knowledge bases leading to informative contamination maps (Savelieva et al. 2005). Exact measurements were combined with secondary local information to assess the uncertainty of soil contamination predictions at unsampled locations. The uncertainty analysis evaluated the ability of the prediction PDF to reproduce the distribution of the raw repeated measurements available in certain populated sites. Moreover, the analysis provided an illustration of the improvement in mapping accuracy obtained by adding soft data to the existing hard data and demonstrated that the BME technique performed well both in terms of prediction accuracy as well as in terms of prediction error assessment, both useful features for the Chernobyl fallout study.

4.4 Cancer distributions associated with Arsenic in Bangladesh drinking water

The occurrence of Arsenic in drinking water is an issue of considerable health interest. In the case of Bangladesh, Arsenic concentrations have been closely monitored since the early 1990s through an extensive sampling network. Human exposure analysis was used to study lifetime population damage due to Arsenic exposure across Bangladesh (Serre et al. 2003). Geographical information science offered powerful tools to assimilate a variety of knowledge bases (physical, epidemiologic, toxicokinetic and demographic) and uncertainty sources (soft data, measurement errors and secondary information). Maps of naturally occurring Arsenic distribution in Bangladesh drinking water were generated. Global indicators of the adverse health effects on the population were derived, and valuable insight was gained by blending information from different scientific disciplines. For illustration, Fig. 15 shows bladder cancer maps (cases per km^2)

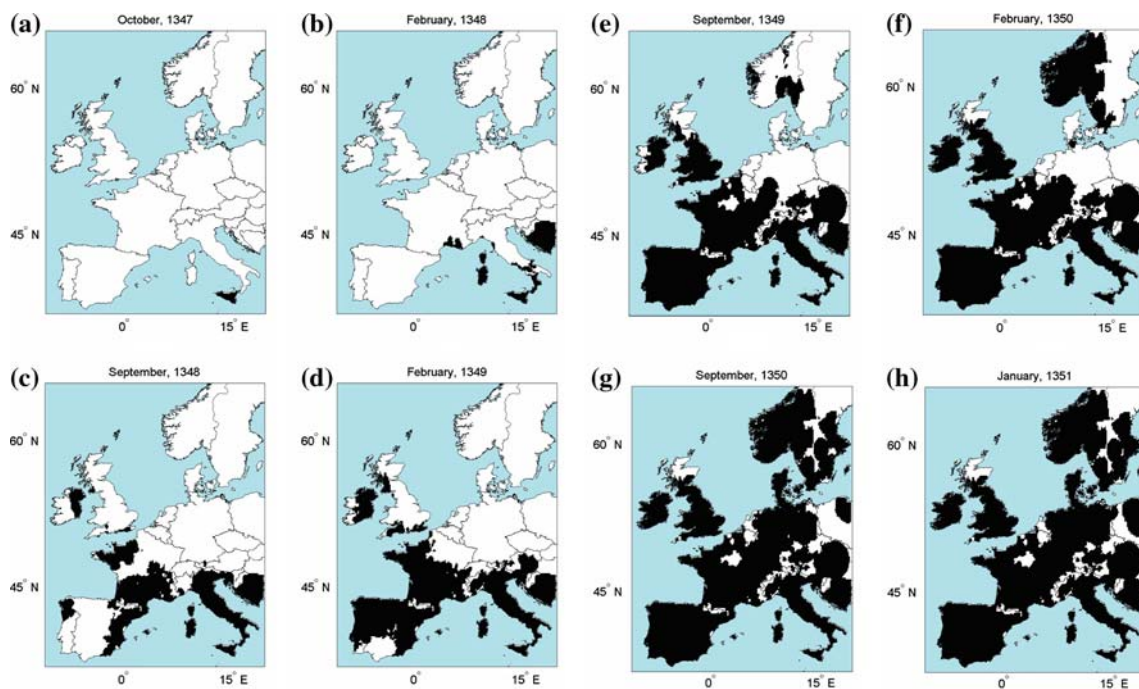


Fig. 13 Total geographical area in Europe infected by Black Death at different times—denoted in *black*

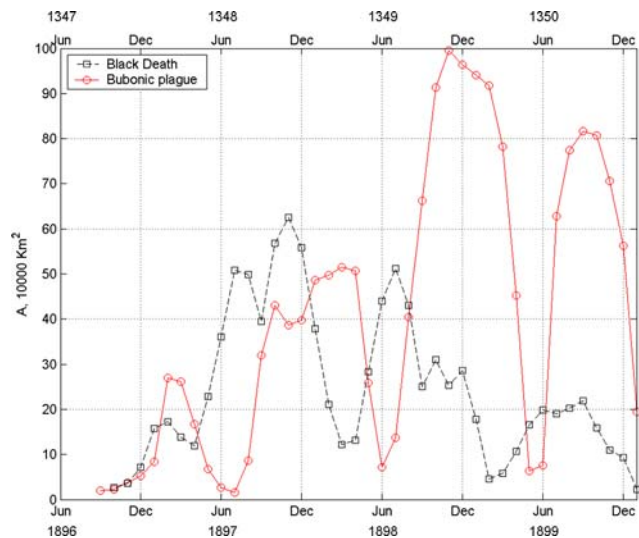


Fig. 14 Geographical extent of infected area, A (in 1,000 km^2) at any given time for the Black Death in Europe and for the bubonic plague in India

obtained by integrating an empirical exposure-response (linear) model versus a multistage carcinogenesis (non-linear) model in the mapping process. In both cases, the results indicated an increased lifetime bladder cancer probability for the Bangladesh population due to Arsenic. The health effect estimates and the associated uncertainty assessments provided valuable tools for a broad spectrum of end-users.

4.5 Patterns of ozone health effects in Eastern USA

Population exposure assessment to potentially harmful pollutants is an important area from both the scientific research and the health management standpoints. In this work the GBME technique was used to study the impact of spatiotemporal ozone exposure distributions on the health of human populations in the eastern USA (Christakos and Kolovos 1999). The spatiotemporal analysis started with exposure distributions producing the input to toxicokinetic laws linked to effect models which, in turn, were integrated with relationships that describe how effects are geographically distributed across populations. The approach emphasized the functional relationships between space-time ozone maps, toxicokinetic models of burden on target organs and tissues, and population health effects. These relationships offered a meaningful interpretation of the exposure and biological processes affecting human exposure. Maps describing possible distributions of exposure, burden and health damage were produced that were associated with “representative” receptors belonging to a specific cohort (e.g., group of people with similar time/activity profiles); see, e.g., Fig. 16 (different cohorts were associated with different sets of maps). These maps can help health scientists and administrators derive valuable conclusions about the expected health effects for a specific population cohort within a specified geographical area and time period.

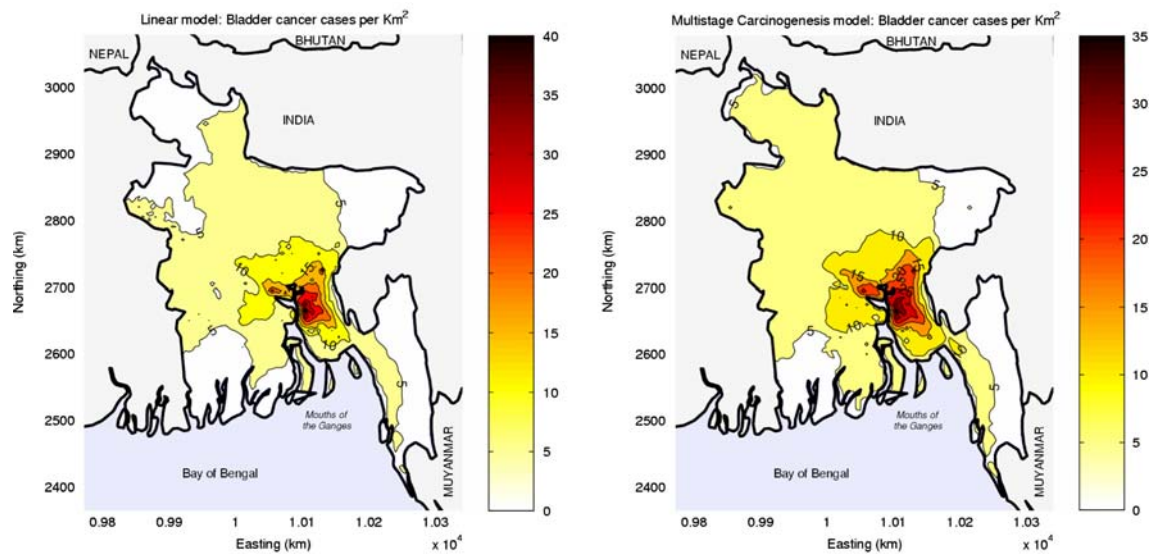


Fig. 15 Bladder cancer maps (cases per km^2) using the empirical exposure-response (linear) model and the multistage carcinogenesis (non-linear) model

4.6 El Niño effects on the influenza mortality risk in California

Recent El Niño events have pointed out the need to develop modelling techniques assessing climate-related health events. Experts agree that climate changes affect the spread of infectious diseases and that the geographic range of infectious diseases might expand as a result of these changes. Nevertheless, the world health modelling community cannot yet predict, with reasonable accuracy, when or where exactly these effects will occur or how large the threat of these diseases will be to particular populations. Choi et al. (2006) compared the spatiotemporal patterns of influenza mortality risk in the state of California during El Niño versus normal weather periods. By focusing on county-specific mortality data, various sources of uncertainty were taken into account and influenza mortality maps and risk profiles were generated. Significant effects of climate change on the influenza risk distributions were detected. Geographical maps of risk variation during El Niño differed from those during normal weather (e.g., Fig. 17), the corresponding covariances exhibited distinct space-time dependence features, and the temporal mean mortality profiles were considerably higher during normal weather than during El Niño. These rather unexpected results of spatiotemporal analysis are worth further investigation that seeks substantive and biologically plausible explanations. The findings of this study offered a methodological framework to evaluate public health management strategies.

4.7 A geographical study of breast cancer dynamics in North Carolina

This work was concerned with the study of breast cancer dynamics in North Carolina, such as incidence variation (Christakos and Lai 1997). The $S/TRF-v/\mu$ model used in this study is significantly general in theory so that it efficiently represented non-homogeneous characteristics of disease variation. Geographical maps provided a detailed quantitative description of the cancer incidence variation throughout the state during various time periods (e.g., Fig. 18). The associated mapping accuracy was also calculated throughout North Carolina and for the specified time periods. The maps offered valuable information about the breast cancer landscape and dynamics in various parts of the state. Field studies could be initialized across a range of high versus low rate areas identified by the maps in an effort to uncover environmental or life-style factors that might be responsible for the high rates; also, the maps can elucidate causal mechanisms at a certain scale, explain disease occurrences and offer guidance in the administration of health services.

4.8 Spatiotemporal analysis of environmental exposure-health effect associations

This work studied causal associations between environmental exposures and health effects by synthesizing sources of physical exposure and population health knowledge (Christakos and Serre 2000). The strength and consistency

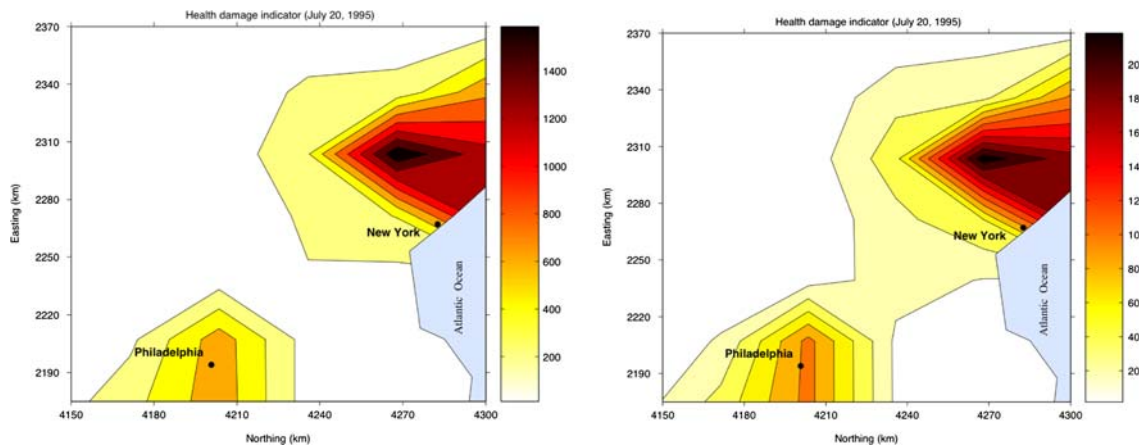


Fig. 16 Maps of the health damage indicator (cases per km²) in the New York city–Philadelphia area on July 20, 1995 due to ozone exposure for two different population cohorts

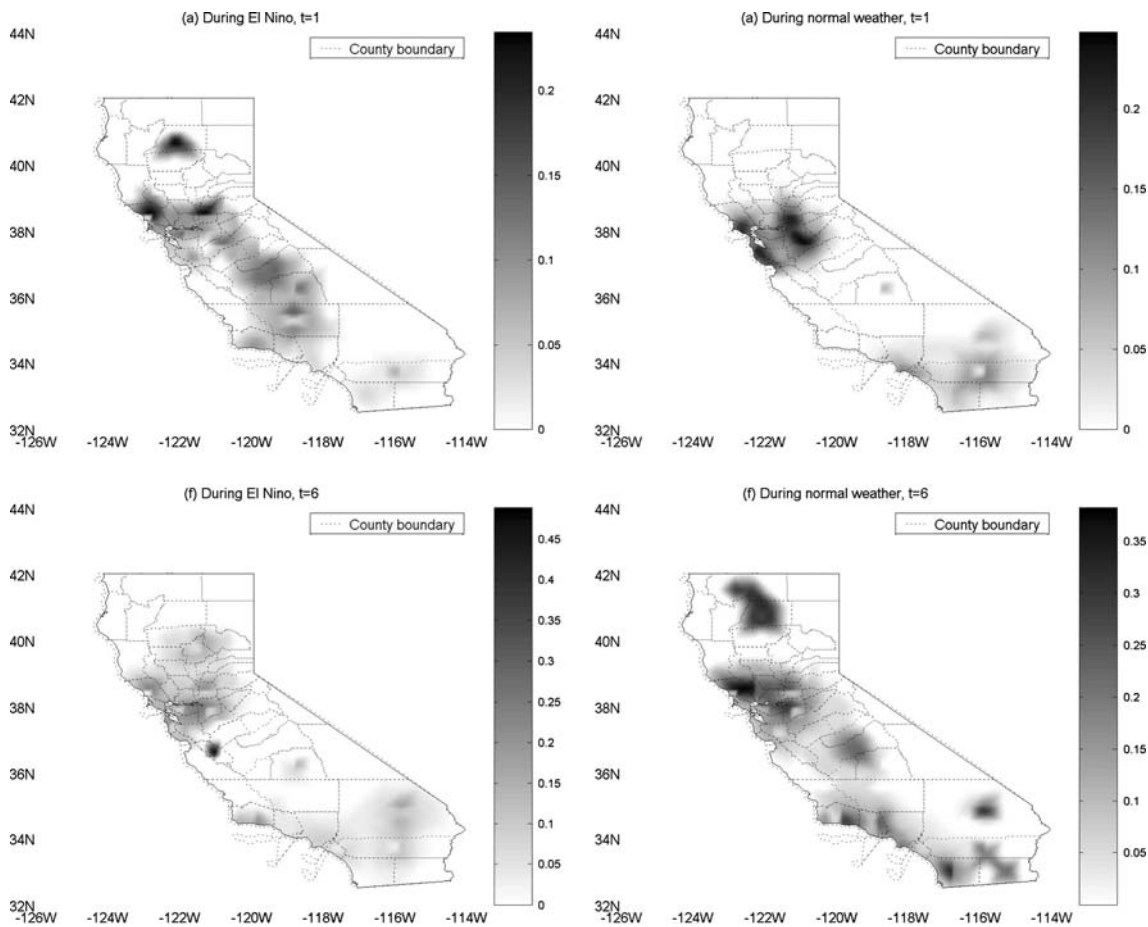


Fig. 17 Risk maps of influenza mortality rates at different times (per 10⁵ individuals of the 65 years or older population group). The *right column* corresponds to the normal weather period and the *left column* to the El Niño period

of the exposure-effect association were evaluated on the basis of health effect predictions that the combined physical-health analysis generated in space-time. A North Carolina study involved mortality (in deaths per 100,000

people per day) and cold temperatures (in °F). The mortality-temperature association was measured by the ratio β_{DX} of the normalized death rate prediction error difference (i.e., death rate prediction error based on both mortality and

temperature information vs. error based on mortality data only). The β_{DX} profile (Fig. 19a) was consistently negative, which supported the existence of a mortality-temperature association (of varying magnitude) during the specified period. The spatial distribution of the association was represented by the β_{DX} map (Fig. 19b), which showed a stronger association in the mountainous area (south-west part of North Carolina); a weaker association occurred at the eastern part of the state and, also, in the urban area near Charlotte. These geographical differences were explained in physical terms; e.g., the moderating influence of the ocean on cold temperatures could explain the weaker effect of the latter along the coastline, and the living conditions (higher exposure to cold temperature in mountainous/rural areas than in urban areas). Accounting for a potential confounder (particulate matter exposure) resulted only in a slightly different strength in the reported mortality-temperature association, thus supporting the view that particulate matter had no significant confounding effect on the resulting association between cold temperature exposure and death rate.

4.9 Efficient mapping of California mortality distributions at different spatial scales

The meaningful characterization of health attributes often involves the assessment of their spatiotemporal variation at multiple scales. In many studies data are available at a larger scale (say, counties), whereas the health geographer is interested in a smaller scale analysis (say, residential neighborhoods). An adequate analysis should depend on the scale at which the attribute is considered, rather than being limited by the scale at which the data are available. Choi et al. (2003) used a BME-based multiscale approach to study California mortality distributions at different geographical scales. Figure 20a is the mortality rate at the county scale (this map did not represent the true rate distribution at the local scale, but rather the rate distribution averaged over a region approximating the size of a county). Then, the mortality rate distribution was derived at the

local scale by means of the multiscale approach (Fig. 20b). Significant differences in the mortality rate distribution can be seen. Figure 20a exhibits smoother patterns, because is limited by the observation scale and the site-specific base used soft data located only at the county centroids. Though this practice is common, it can lead to artificial patterns (the maps exhibit islands of either high or low values around the centroids). On the other hand, the multiscale approach did not suffer from these limitations. In order to filter out artificial effects, it used a BME feature that processes soft information at the data points themselves. The generated map (Fig. 20b) displayed more variability at the local scale, whereas the artificial features around the county centroids have been toned down; the contours lines of mortality rate followed more the outline of county boundaries (for which the information was collected), rather than the centroid locations (which were arbitrary choices). Accuracy measures demonstrated that the multiscale approach offered more accurate mortality predictions at the local scale than existing approaches that did not account for scale effects (an error reduction of up to 20% relative to the predictions of the scale-free approach was found). Hence, depending on the data characteristics and the purpose of the health study, the multiscale mapping approach can be used to generate accurate and informative maps at any scale of interest, without restriction to the scale of the measurement.

5 Discussion

The SEKS-GUI toolkit allows health scientists, interdisciplinary knowledge synthesis experts and spatiotemporal statisticians, among others, to blend different knowledge bases in a rigorous way and generate a variety of space-time predictive maps of considerable scientific value. Dealing with the lives of humans, it is only natural for researchers to be rigorous and open to different types of information, as well as transparent in the communication of their prediction uncertainty.

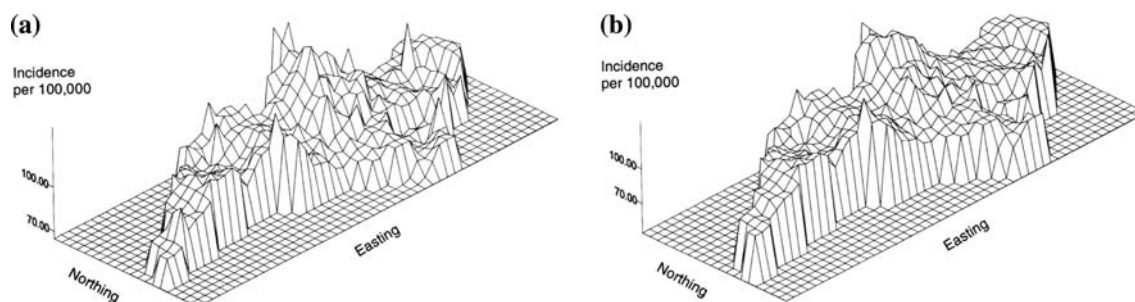


Fig. 18 North Carolina breast cancer incidence maps in the year **a** 1991 and **b** 1992

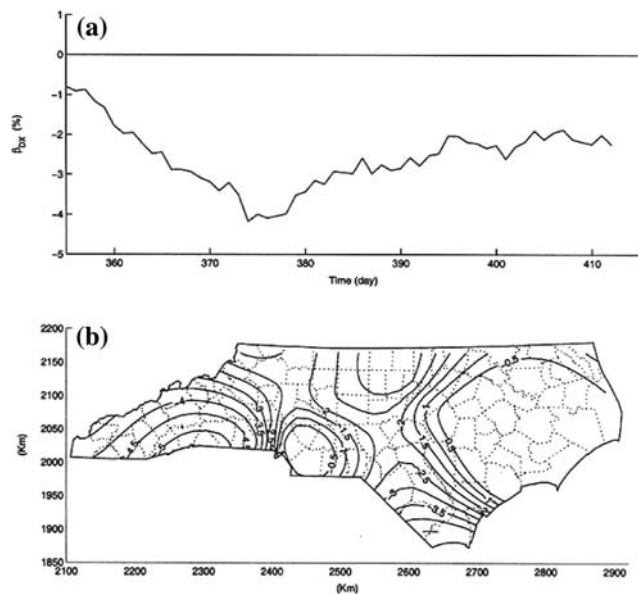


Fig. 19 **a** Time profile and **b** spatial map of β_{DX} (in %); winter of 1996

The use of knowledge synthesis in the medical geography discipline utilizes powerful analytical and computational methods that incorporate knowledge that would otherwise be dismissed and is more informative than other GIS software since it generates the complete probability distribution at each point in space–time. By incorporating space–time dependency representations under conditions of uncertainty, researchers are able to characterize patterns and processes with far greater prediction accuracy and error assessment. This work focuses on innovative implementation of knowledge synthesis research using the SEKS–GUI computer software library, a user-friendly interface that allows users to focus on the substantive

problem at hand without becoming mired into programming and data transformation details. The tools and theory of SEKS–GUI have been available previously, yet now the GUI front end of the toolkit allows even non-experts to explore their data in novel ways. The techniques of spatiotemporal analysis field are powerful and sophisticated. The usage of spatiotemporal analysis techniques in the practical health policy arena may be far from matching their potential value. Nevertheless, the GUI front end to SEKS is an attempt to address this gap.

The SEKS–GUI enables users to account for spatiotemporal heterogeneous dependence, non-Gaussian probability laws, non-linear predictors and operational data assimilation, and to generate complete PDF (uni- and multi-variate) at all mapping grid nodes. In this work, we focus on two of the techniques available: BME and GBME, both of which incorporate general (core) and site-specific knowledge bases, including hard (certain) and soft (uncertain) data (unique to SEKS–GUI is an ability to process soft information at the mapping grid nodes, as well). Through a series of detailed screens—from data input and exploration to spatiotemporal covariance analysis and prediction—the user arrives at the visualization stage where a wide variety of maps are available to add insight into the spatiotemporal characteristics of the health system.

A series of real-world case studies were presented to give the reader a clear picture of the SEKS–GUI efficiency and versatility, as well as the valuable insights and improved results obtained in terms of the SEKS–GUI (composite space–time maps of the health attributes, accuracy analysis, risk assessment distributions etc.).

The SEKS–GUI will evolve as future needs present themselves; new space–time covariance models will be included; vector attributes (i.e., the space–time modeling and mapping of several health-related attributes simulta-

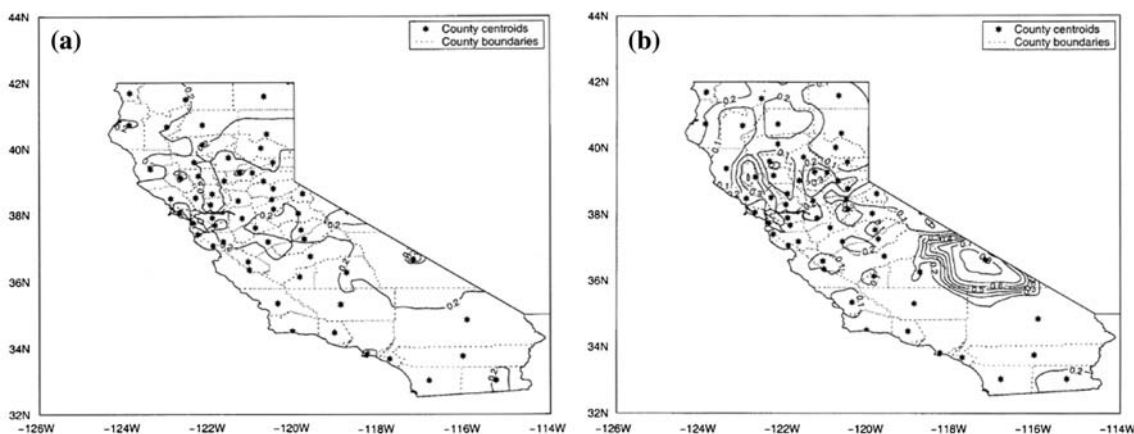


Fig. 20 Map of spatial distribution of mortality rate (death per 100,00 people per day) in California on January 1, 1989, **a** at the county scale, **b** at the local scale (multiscale approach)

neously) will be taken into account; other kinds of spatiotemporal predictors will be included, like the MBME and GMBME (Table 3); and new core knowledge bases will be assimilated (physical laws, health models, scientific theories etc.). More vivid and descriptive maps can be created, when more knowledge bases (physical, epidemiologic, demographic, secondary information etc.) are assimilated into modeling. SEKS-GUI provides a relatively straightforward framework by which to achieve this goal.

Acknowledgments The research was supported by grants from the Fred J. Hansen Institute (Grant No. 54266A P3590), the Oak Ridge National Lab (OR7865-001.01), and the National Institute of Environmental Health Sciences (P30ES10126).

Appendix A: The case of co-located data at Phase 2

Because duplicate coordinates (co-located data) may result in covariance matrix singularities, an initial check for duplicates is performed. The same adverse effect may occur at the prediction phase when geographical data are very close to each other. Co-location is not necessary associated with common public health problems in which a common geocode is assigned to participants with missing/incomplete addresses or to those residing in a specified geographic region to assure confidentiality. The interface defines the degree of proximity with respect to the geographical extent of the dataset and treats data that are too close to each other as co-located. Many methods may be used to alleviate the co-location issue, among them value averaging, slight spatial data displacement, and choosing a datum as the representative value of the co-located dataset. Another possibility is to merge co-located hard data into a unique soft data interval ranging within the span of the co-located hard data values. To preserve the character of the user's dataset, the SEKS-GUI performs a simple averaging of the co-located hard data values and deals with co-location of soft uncertain data with other soft or hard data by means of slight random displacements.

Appendix B: Transformation options at Phase 2

By way of a summary, SEKS-GUI offers the following transformation options:

- (a) *No transformation*. The detrended dataset is left unaltered and the user proceeds to the prediction phase with the data in their original space.
- (b) *N-scores transformation* (also known as normal scores or Gaussian anamorphosis; Olea 1999). The detrended dataset is transformed to a $N(0, 1)$ Gaussian

distribution and the resulting dataset (used in space-time prediction) lies in the N -score space. Back-transformation to the original space is possible by using the N -score matrix. Since some extreme values may not back-transform properly using the N -score matrix, the SEKS-GUI sets upper and lower transformation limits that depend on the data span of the particular study, thus providing a means for extreme predictions to be appropriately back-transformed. All the N -score transformation functions are automatic and seamless to the user.

- (c) *Box-Cox transformation* (Box et al. 1994). The detrended dataset is tested with a series of power transformations based on a λ -parameter typically ranging within ± 2 . The transformation eventually uses the λ -value bringing the data distribution closest to a Gaussian one. The resulting data values to be used in prediction are in the Box-Cox space. The back-transformation depends on the optimal λ -value chosen for the specific dataset. Note that the Box-Cox transformation is defined for positive data values only, while the detrended data will likely feature negative or zero values. If negative values are present, a constant is added to the detrended set so that all transformed values are positive. After being back-transformed to the original space, the constant is removed. The interface also accounts for the possibility of zero values (which pose problems when calculating logarithms). The above functions are performed automatically and are seamless to the user.

Appendix C: The BME and GBME techniques

Some of the implementation differences between BME and GBME are briefly discussed below (for more information about the two theories and technical details, the interested reader is referred to the relevant literature).

The two techniques may use different modelling assumptions and emphasize distinct core knowledge bases. For practical reasons, BME studies heterogeneity in an indirect way: it assumes a decomposition of the original attribute distribution into a mean function and a residual attribute, and a transformation operator is applied to the residual before BME is implemented. GBME theory deals directly with attribute heterogeneity in terms of space-time increments of the original distribution. Accordingly, the numerical implementation of GBME requires fewer steps than BME and its implementation is intrinsic, to a considerable extent. On the other hand, the BME steps are explicit, often allowing an increased participation of the user. GBME provides information about the space-time

dependence structure in terms of the heterogeneity orders, which are not available in BME. GBME correlation analysis focuses on a local space–time scale at each prediction point, whereas BME analysis applies at a larger geographical scale that includes several prediction points. Accordingly, the GBME should perform best when enough data points are available at each local scale. On the other hand, there are more data points available at the BME scale, often generating smoother maps. While BME uses ordinary covariance functions that need to be positive-definite, GBME uses generalized covariance functions that need to be only conditionally positive-definite. Under certain conditions, the user may consider the implementation of a combination of BME and GBME, i.e., a decision is made to apply the BME technique in some sub-regions of the study area and the GBME technique in some others.

References

- Bogaert P (1996) Comparison of kriging techniques in a space–time context. *Math Geol* 28(1):73–86
- Box GEP, Jenkins GM, Reinsel GC (1994) *Time series analysis, forecasting and control*, 3rd edn. Prentice Hall, Englewood Cliffs
- Choi K-M, Serre ML, Christakos G (2003) Efficient mapping of California mortality fields at different spatial scales. *J Expo Anal Environ Epidemiol* 13(2):120–133
- Choi K-M, Christakos G, Wilson ML (2006) El Niño effects on influenza mortality risks in the state of California. *J Public Health* 120:505–516
- Christakos G (1990) *Random field modelling and its applications in stochastic data processing*. Ph.D. Thesis, Division of Applied Sciences, Harvard University, Cambridge, MA
- Christakos G (1991) On certain classes of spatiotemporal random fields with application to space–time data processing. *IEEE Trans Syst Man Cybern* 21(4):861–875
- Christakos G (1992) *Random field models in earth sciences*. Acad Press, San Diego. New edition, Dover Publishing Inc., Mineola, NY, 2005
- Christakos G (2000) *Modern spatiotemporal geostatistics*. Oxford University Press, New York
- Christakos G, Bogaert P (1996) Spatiotemporal analysis of spring-water ion processes derived from measurements at the Dyle Basin in Belgium. *IEEE Trans Geosci Remote Sens* 34(3):626–642
- Christakos G, Hristopulos DT (1998) *Spatiotemporal environmental health modelling*. Kluwer, Boston
- Christakos G, Kolovos A (1999) A study of the spatiotemporal health impacts of ozone exposure. *J Expo Anal Environ Epidemiol* 9(4):322–335
- Christakos G, Lai J (1997) A study of the breast cancer dynamics in North Carolina. *Soc Sci Med D Med Geogr* 45(10):1503–1517
- Christakos G, Bogaert P, Serre ML (2002) *Temporal GIS*. Springer, New York (with CD-ROM)
- Christakos G, Kolovos A, Serre ML, Vukovich F (2004) Total ozone mapping by integrating data bases from remote sensing instruments and empirical models. *Geosci Remote Sens* 42(5):991–1008
- Christakos G, Olea RA, Serre ML, Yu HL, Wang L-L (2005) *Interdisciplinary public health reasoning and epidemic modeling: the case of black death*. Springer, New York
- Christakos G, Olea RA, Yu H-L (2007) Recent results on the spatiotemporal modelling and comparative analysis of Black Death and Bubonic Plague epidemics. *J Public Health* (in press)
- Cressie N, Huang HC (1999) Classes of nonseparable, spatio-temporal stationary covariance functions. *J Am Stat Assoc* 94:1330–1340
- Cromley EK, McLafferty SL (2002) *GIS and public health*. The Guilford Press, New York
- Douaik A, Van Meirvenne M, Tóth T, Serre ML (2004) Space–time mapping of soil salinity using probabilistic Bayesian maximum entropy. *Stoch Environ Res Risk Assess* 18:219–227
- Douaik A, Van Meirvenne M, Toth T (2005) Soil salinity mapping using spatio-temporal kriging and Bayesian maximum entropy with interval soft data. *Geoderma* 128:234–248
- Ebi KL, Smith J, Burton I (2005) *Integration of public health with adaptation to climate change*. Taylor & Francis, Oxford
- Gatrell AC (2002) *Geographies of Health*. Blackwell, Malden
- Goodall C, Mardia KV (1994) Challenges in multivariate spatio-temporal modeling. In *Proceedings of the XVIIth International Biometric Conference*, 1–17, August 8–12, 1994, Hamilton, Ontario, Canada
- Haas TC (1995) Local prediction of spatio-temporal process with an application to wet sulfate deposition. *J Am Stat Assoc* 90:1189–1199
- Haggett P (2000) *The geographical structure of epidemics*. Clarendon Press, Oxford
- Keil FC, Wilson RA (eds) (2000) *Explanation and cognition*. The MIT Press, Cambridge
- Knorr Cetina K (1999) *Epistemic cultures: how the sciences make knowledge*. Harvard University Press, Cambridge
- Kolovos A, Christakos G, Serre ML, Miller CT (2002) Computational BME solution of a stochastic advection-reaction equation in the light of site-specific information. *Water Resour Res* 38(12):1318–1334
- Kolovos A, Christakos G, Hristopulos DT, Serre ML (2004) Methods for generating non-separable spatiotemporal covariance models with potential environmental applications. *Adv Water Resour* 27:815–830
- Kolovos A, Yu H-L, Christakos G (2006) SEKS–GUI v.0.6 user manual. Department of Geography, San Diego State University, San Diego
- Kyriakidis PC, Journel AG (1999) Geostatistical space–time models: a review. *Math Geol* 31(6):651–684
- Law DCG, Bernstein K, Serre ML, Schumacher CM, Leone PA, Zenilman JM, Miller WC, Rompalo AM (2006) Modeling an early syphilis outbreak through space and time using the Bayesian maximum entropy approach. *Ann Epidemiol* 16(11):797–804
- Ma C (2003) Spatio-temporal stationary covariance models. *J Multivariate Anal* 86:97–107
- Meyer J-JCh, Van Der Hoek W (2004) *Epistemic logic for AI and computer science*. Cambridge University Press, Cambridge
- Olea RA (1999) *Geostatistics for engineers and earth scientists*. Kluwer, Boston
- Olea R (2006) A six-step practical approach to semivariogram modeling. *J Stoch Environ Res Risk Assess* 20(5):1436–3240
- Orton TG, Lark RM (2007) Accounting for the uncertainty in the local mean in spatial prediction by BME. *J Stoch Environ Res Risk Assess* 21 (in press)
- Quilfen Y, Chapron B, Collard F, Serre ML (2004) Calibration/validation of an altimeter wave period model and application to TOPEX/Poseidon and Jason-1 Altimeters. *Marine Geodesy* 27:535–550
- Rescher N (2005) *Epistemic logic: a survey of the logic of knowledge*. University of Pittsburgh Press, Pittsburgh

- Savelieva E, Demyanov V, Kanevski M, Serre ML, Christakos G (2005) BME-based uncertainty assessment of the Chernobyl fallout. *Geoderma* 128:312–324
- Serre ML, Christakos G (1999) Modern geostatistics: computational BME in the light of uncertain physical knowledge—the Equus Beds study. *Stoch Environ Res Risk Assess* 13(1):1–26
- Serre ML, Bogaert P, Christakos G (1998) Computational investigations of Bayesian maximum entropy spatiotemporal mapping. In: Buccianti A, Nardi G, Potenza R (eds) 4th Annual Conference, vol 1, De Frede Editore, Naples, Italy, pp 117–122
- Serre ML, Kolovos A, Christakos G, Modis K (2003) An application of the holistochastic human exposure methodology to naturally occurring Arsenic in Bangladesh drinking water. *Risk Anal* 23(3):515–528
- Stein ML (2005) Space–time covariance functions. *J Am Stat Assoc* 100:310–321
- Wibrin M-A, Bogaert P, Fasbender D (2006) Combining categorical and continuous spatial information within the Bayesian maximum entropy paradigm. *Stoch Environ Res Risk Assess* 20:423–434
- Yu H-L, Christakos G (2006) Spatiotemporal modelling and mapping of the bubonic plague epidemic in India. *Int J Health Geogr, Online Journal* 5(12). <http://www.ij-healthgeographics.com/content/5/1/12>